

Non-universal level statistics in a chaotic quantum spin chain

Carlos Pineda^{1,2,3,*} and Tomaž Prosen^{4,†}

¹*Instituto de Ciencias Físicas, Universidad Nacional Autónoma de México, México*

²*Instituto de Física, Universidad Nacional Autónoma de México, México*

³*Centro Internacional de Ciencias, Cuernavaca, México*

⁴*Physics Department, Faculty of Mathematics and Physics, University of Ljubljana, Ljubljana, Slovenia*

(Dated: October 14, 2018)

We study the level statistics of an interacting multi-qubit system, namely the kicked Ising spin chain, in the regime of quantum chaos. Long range quasi-energy level statistics show effects analogous to the ones observed in semi-classical systems due to the presence of classical periodic orbits, while short range level statistics display perfect statistical agreement with random matrix theory. Even though our system possesses no classical limit, our result suggest existence of an important non-universal system specific behavior at short time scale, which clearly goes beyond finite size effects in random matrix theory.

PACS numbers: 05.30.-d,05.45.Mt,05.45.Pq

I. INTRODUCTION

One of the key discoveries of quantum chaos has been the so-called quantum chaos conjecture, originally proposed in Refs. [1]. It claims that even simple non-integrable quantum systems, whose dynamics is sufficiently complex (say, dynamically mixing in the classical limit), possess quantum fluctuations which can be described by a universal ensemble of random matrices without any free parameters [2]. Although a strict mathematical proof of this conjecture is still missing, its theoretical understanding has recently been considerably deepened [3]. Still, it is known from the early years of quantum chaos [4], that level fluctuations exhibit universal features only on sufficiently small energy scales, or long time scales, whereas one obtains system specific non-universal features on long energy scales (short time-scales) which can be usually understood and computed in terms of classical orbits.

Therefore it seems that the picture is quite complete and satisfactory for systems possessing a well defined classical limit. But what about simple systems which do not have a classical limit, e.g., systems of interacting fermions, or systems of interacting qubits? In such systems, dynamical complexity can be reached in the thermodynamic limit of many interacting particles [5]. In some exactly solvable cases formal similarities between the thermodynamic limit and the semi-classical limit can be established [6]. For example, one may start by considering simple, *non-integrable*, many-particle Hamiltonians with local interaction which are specified by only a few (*non-random*) parameters. Can quantum spectral fluctuations of such systems be described by universal ensembles of random matrices? If yes, what are the energy scales of such universality? Is there a breaking of univer-

ality at sufficiently large energy ranges? How does the universality breaking scale in the thermodynamic limit? In this paper we address these questions in a simple dynamical system, namely an Ising chain of spin 1/2 particles on a 1d ring, kicked periodically with a homogeneous, tilted magnetic field. We performed careful numerical calculations of quasi-energy spectra and their statistical analysis. For appropriate values of model's parameters, corresponding to strong integrability breaking, we indeed find both, the *universality regime* for sufficiently small energy scales, where no statistically significant deviations from random matrix prediction of infinitely dimensional Circular Orthogonal Ensemble (COE) could be detected, and a *non-universality regime* for large energy scales (or small times, corresponding to few kicks), where clear, statistically significant deviations from Random Matrix Theory (RMT) prediction have been found. Most notably, our analysis shows that the spectral form factor exhibits significant deviations from RMT at the time scale corresponding to one or few kicks (Floquet periods). This result could be intuitively understood as a qubit analogy of “shortest periodic orbit” correction, but its precise theoretical understanding is at present open.

II. THE SYSTEM

The system we study is a *kicked Ising chain* (KIC) [7], namely a ring of L spin 1/2 particles which interact with their nearest neighbors via a homogeneous Ising interaction of dimensionless strength J and being periodically kicked with a homogeneous magnetic field of dimensionless strength \vec{b} . During the free evolution, *i.e.* between the kicks, the system evolves with the unitary propagator

$$U_{\text{Ising}}(J) = \exp \left(-iJ \sum_{j=0}^{L-1} \sigma_j^z \sigma_{j+1}^z \right), \quad (1)$$

*Electronic address: carlospgmat03@gmail.com

†Electronic address: tomaz.prosen@fmf.uni-lj.si

and the action of the kick is described by the unitary operator

$$U_{\text{kick}}(\vec{b}) = \exp\left(-i \sum_{j=0}^{L-1} \vec{b} \cdot \vec{\sigma}_j\right), \quad (2)$$

with $\sigma_j^{x,y,z}$ being the Pauli matrices of particle j and $\vec{\sigma}_j = (\sigma_j^x, \sigma_j^y, \sigma_j^z)$. The Floquet operator for one period is thus

$$U_{\text{KI}} = U_{\text{Ising}}(J)U_{\text{kick}}(\vec{b}). \quad (3)$$

We must also impose periodic conditions in order to close the ring: $\vec{\sigma}_L \equiv \vec{\sigma}_0$. During this paper we shall use the so called computational basis, which is composed of joint eigenstates of σ_j^z . This set of basis states can be written as $S = \{|m_0 m_1 \dots m_{L-1}\rangle$, with $m_j \in \{0, 1\}$.

In order to understand the spectrum one must first discuss the symmetries in the system. Let us start with the translational symmetry. The corresponding operator T is defined on the computational basis as $T|m_0 m_1 \dots m_{L-1}\rangle = |m_{L-1} m_0 \dots m_{L-2}\rangle$, and is extended to the entire Hilbert space by linearity. The action of this operator is to rotate the particles in the ring by one site. The eigenvalues of T are $\exp(2\pi i k/L)$ with $k \in \mathbb{Z}/L$. Hence the Hilbert space is foliated into L subspaces $\mathcal{H} = \bigoplus_{k \in \mathbb{Z}/L} \mathcal{H}_k$. The evaluation of the dimensionality of each of these subspaces is described in Appendix A. The evolution operator (3) is translationally invariant, and hence $[U_{\text{KI}}, T] = 0$.

The next symmetry is an external reflection R . Its action on the basis S reads $R|m_0 m_1 \dots m_{L-1}\rangle = |m_{L-1} m_{L-2} \dots m_0\rangle$, and also $[U_{\text{KI}}, R] = 0$. The two symmetries, T and R , do not commute. It must be noticed that if $|\psi\rangle \in \mathcal{H}_k$, then $R|\psi\rangle \in \mathcal{H}_{-k}$. This provides an additional symmetry within the subspace \mathcal{H}_0 (and $\mathcal{H}_{L/2}$ for even L). Thus these marginal subspaces are regarded as “special” and have slightly different properties than the rest. We shall not consider them for the purpose of statistical analysis in this article.

Finally, we define the anti-unitary symmetry \mathcal{K}' . It acts as a mirror reflection within each spin with respect to the plane that contains both \vec{b} and the unitary vector in the z direction (the direction of the Ising interaction). We can rotate our coordinate system around the z axis in each qubit so that \vec{b} only has components in the x and z directions. Then, \mathcal{K}' is simply complex conjugation, provided that σ_x and σ_z are set real, as is the usual choice. This symmetry operation also changes the sign of the momentum. Composing $\mathcal{K} = \mathcal{K}'R$, we arrive to an anti-unitary symmetry that preserves the momentum *i.e.* an anti-unitary symmetry within each \mathcal{H}_k .

Concluding, U_{KI} has a rotational symmetry R that foliates the spectrum into L different sectors; the sector k has identical spectrum as the sector $-k$. Hence for a fixed number of qubits we expect to have a maximum of $(L-1)/2$ relevant sectors, each sector having a Hilbert space dimension $\mathcal{N} \approx 2^L/L$. Since each sector

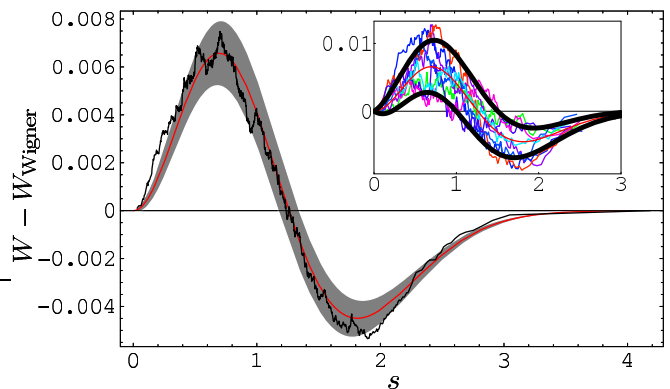


FIG. 1: (Color online) We study the behavior of the integrated nearest neighbor spacing distribution, $W(s)$. The noisy curve shows the difference between the numerical data for 18 qubits, averaged over the different relevant \mathcal{H}_k spaces, and the Wigner surmise. The smooth (red) curve is the difference between infinitely dimensional COE solution and the Wigner surmise. The expected standard deviation due to the finite size of the spectrum σ_W [see Eq. (4)] is also indicated as the shaded area surrounding the RMT result. In the inset we present a similar figure with the results for each of the \mathcal{H}_k subspaces plotted separately, together with the error associated with each individual spectrum, as the thick black curves. (Different colors represent different sectors, according to the coding shown in Fig. 3.)

has an internal anti-unitary symmetry, we shall compare the statistical properties of system’s spectrum to those of Dyson’s Circular Orthogonal Ensemble [2] of random matrices, of appropriate dimension.

For the rest of the presentation we fix parameter values of our system $J = 0.7$, $\vec{b} = (0.9, 0, 0.9)$ for which the integrability of the model is strongly broken. We believe that for these parameter values the system is a generic representative of quantum chaos. Using highly optimized numerical methods (see appendix B) we have been able to diagonalize the model accurately for sizes up to $L = 18$ qubits. The eigenvalues of the Floquet propagator U_{KI} have been written as $\exp(-i\varphi_n)$, where φ_n are known as quasi-energies, and have been grouped with respect to the known quasi-momentum k . Statistical analyses of desymmetrized quasi-energy spectra $\{\varphi_n\}$ and their interpretation are given in the following sections. In order to compare with the RMT formulae we normalize the quasi-energies, *i.e.* write $s_n = \frac{\mathcal{N}}{2\pi}\varphi_n$, in order to have mean level spacing equal to one (\mathcal{N} denotes the dimension of the Hilbert space). Similarly, $s = \frac{\mathcal{N}}{2\pi}\varphi$ will denote the spectral variable, unfolded to a unit mean level spacing.

III. UNIVERSALITY REGIME

Let us first analyze the most commonly studied spectral statistics of chaotic systems, that is the nearest

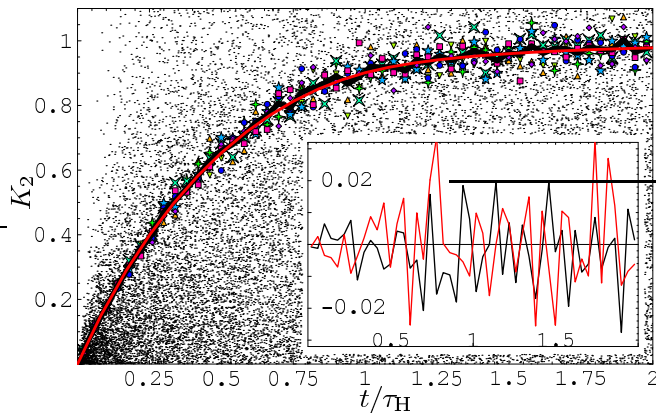


FIG. 2: (Color online) In this plot we show the behavior of the form factor for 18 qubits. The black dots show its value at integer times for the quasi-momentum sector $k = 1$. In order to appreciate clearly its behavior it is necessary to perform a windowing over short ranges of time ($\tau_H/25$). The results for each of the k -spaces are shown according to the symbol scheme in Fig. 3. The average over the different spaces as well as the theoretical curve is plotted as a black and red line, respectively. In order to compare with the ensemble fluctuations, we plot in the inset the difference from the theoretical prediction of both, the spectra for the KIC (in black), and the spectra of an equal number of random realizations of COE members with the same dimension (in red).

neighbor level spacing distribution $P(s)$. $P(s)ds$ is the probability that the distance between two nearby (unfolded) quasi-energies is between s and $s + ds$. $P(s)$ has been computed for the KIC and compared to the exact random matrix COE result (computed from Pade approximants [8]) with satisfactory results (not shown). However, since the details of such plot depend on the size of the binning of histograms, we prefer to show the cumulative (integrated) level spacing distribution $W(s) = \int_0^s ds' P(s')$. In fig. 1 we show a comparison of $W(s)$, both for the KIC and the exact infinitely-dimensional COE result, with the Wigner surmise $W_{\text{Wigner}}(s) = 1 - \exp(-\pi s^2/4)$. The expected statistical fluctuation of cumulative probability can be estimated [9] as

$$\sigma_W = \sqrt{\frac{W(1-W)}{\mathcal{N}}} \quad (4)$$

and gives a very realistic estimate of actual fluctuations of our dynamical system. We plot the results both for individual quasi-momentum k subspaces, and averaged over all k . In conclusion, based on the nearest neighbor level spacing distribution we find no significant deviations from universality, i.e. from COE model statistics.

Further on, we have studied other statistical measures of quasi-energy spectra, which are more sensitive to long-range spectral correlations, namely the number variance and the form factor [2]. The spectral form factor K_2 , is defined for discrete time t as $K_2(t/\tau_H) = |\text{Tr } U^t|^2/\mathcal{N}$,

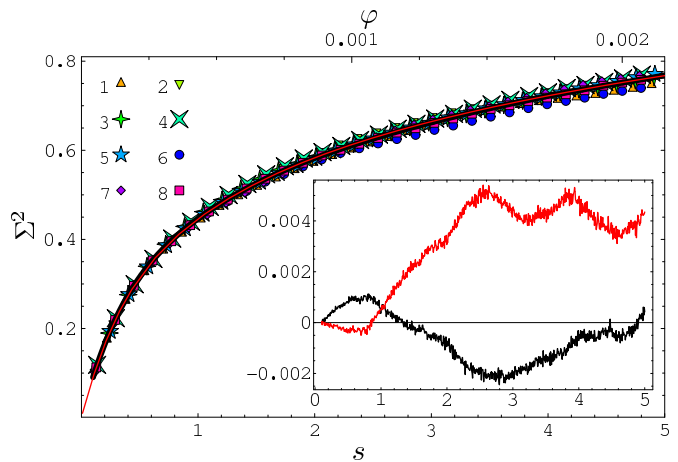


FIG. 3: (Color online) We observe the variance Σ^2 for each symmetry sector (as different symbols) and its average (thick black curve), for 18 qubits. Note that lower abscissa indicates the unfolded spectral variable, while the upper abscissa the one without unfolding. The average curve is almost indistinguishable from the theoretical value (thin red curve). In the inset we compare the deviation of the averaged Σ^2 for both the KIC (in black) and the COE (in red) from the theoretical value Σ_{COE}^2 . No qualitative difference is observed.

and for infinitely dimensional COE has the form

$$K_{2,\text{COE}}(\tau) = \begin{cases} 2|\tau| - |\tau| \ln(2|\tau| + 1) & \text{if } |\tau| < 1 \\ 2 - |\tau| \ln \frac{2|\tau|+1}{2|\tau|-1} & \text{if } |\tau| \geq 1 \end{cases} \quad (5)$$

$\tau_H = \mathcal{N}$ denotes the discrete Heisenberg time, namely the number of kicks in which the average quasi-energy level separation grows to 2π . Asymptotic finite dimension corrections to the form factor have been computed, and for small $\tau \ll 1$, the result reads

$$K_{2,\text{COE}}(\tau, \mathcal{N}) = \left[1 + \frac{1}{\mathcal{N}} + \mathcal{O}(\mathcal{N}^{-2}) \right] K_{2,\text{COE}}(\tau). \quad (6)$$

The number variance $\Sigma^2(s)$ gives the variance of the number of levels in an unfolded spectral interval of length s . The RMT formula for infinitely dimensional COE predicts a monotonically increasing variance $\Sigma_{\text{COE}}^2(s) = (2/\pi^2)[\ln(2\pi s) + 1 + \gamma - \pi^2/8] + \mathcal{O}(s^{-1})$, where $\gamma = 0.5772\dots$ is the Euler constant [2]. However, for a finite spectrum of \mathcal{N} quasi-energy levels this is not possible, since when the energy difference reaches the range of the spectrum the number of levels counted will always be the maximum and hence the number variance will be zero. For arbitrary finite dimension \mathcal{N} , there is an exact relationship [10] between Σ^2 and K_2 that accounts for the finite range of the spectrum:

$$\Sigma^2(s, \mathcal{N}) = \frac{2\mathcal{N}}{\pi^2} \sum_{m=1}^{\infty} \frac{1}{m^2} \sin^2\left(\frac{m\pi s}{\mathcal{N}}\right) K_2\left(\frac{m}{\tau_H}\right). \quad (7)$$

Truncating the above series at finite m with the form

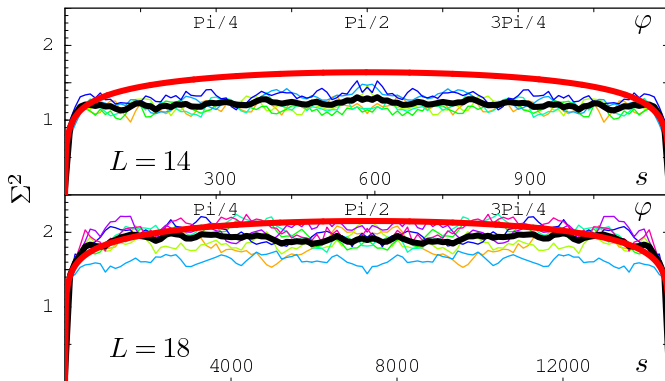


FIG. 4: We plot Σ^2 for the KIC for $L = 14$ (upper plot) and $L = 18$ (lower plot). Different sectors are plotted using thin colored curves (with the same color coding as in Fig. 3) and the average value as the thick black curve. The theoretical (COE) prediction for \mathcal{N} dimensional circular random matrices [eq. (7)] is also plotted as a smooth red curve. We observe saturation of the stiffness for the KIC, characteristic of semi-classical systems.

factor given by eq. (6) provides an excellent asymptotic approximation to the COE number variance for finite \mathcal{N} .

In figure 2 we compare the spectral form factor of the KIC with the infinitely dimensional COE, on a global time scale (on the order of Heisenberg time $\tau_H = \mathcal{N}$). Of course, since the form factor is not self-averaging we had to perform some averaging over short time-windows in order to wash away the statistical fluctuations. We find no notable deviation from the COE. In order to estimate the expected fluctuations due to a finite sample of systems (namely a set of $\approx L/2$ quasi-momenta k) we have also generated a similar average over the same number of random matrices of equivalent size. In the inset we plot the deviations of the form factor computed for the KIC, and the corresponding finite average over random members of the COE, from the exact RMT prediction. We observe that both behave similarly. In addition, we find very good agreement for the number variance Σ^2 of the KIC with the infinitely dimensional COE on short and intermediate spectral ranges $s < 10$ (see fig. 3). In the inset the finite size fluctuations are also compared with the ones computed from appropriate finite samples of finite dimensional COE. Again we observe agreement.

IV. DEVIATIONS FROM UNIVERSALITY

As explained in the previous section, we expect that the number variance for a finite spectrum reaches a maximal value at $\varphi = \pi$ (i.e. $s \sim \mathcal{N}/2$). Actually as already mentioned, one can compute a good analytical approximation to COE averages of number variance for finite \mathcal{N} using eq. (7), and the saturation can be understood as a consequence of discreteness of time in the sine-like transformation on the RHS of (7).

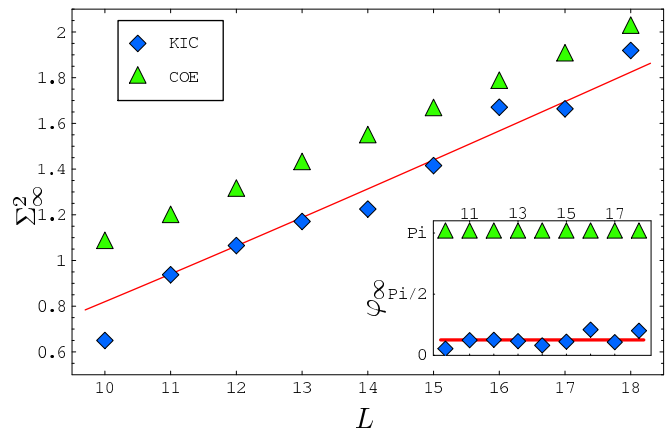


FIG. 5: (Color online) We see the dependence of Σ_∞^2 as a function of the number of qubits L , both for the KIC and the COE of appropriate dimension. In the inset we plot φ_∞ . The constant line $\varphi_c = 0.39$ is shown in red, as well the plot of $\Sigma_{\text{COE}}^2(\mathcal{N}\varphi_c/2\pi, \mathcal{N})$ in the main panel.

Do the spectra of KIC in the regime of quantum chaos follow the same saturation as would be expected for typical members of the COE or not? We have performed detailed numerical checks of these questions and report the results in the following figures. In fig. 4 we plot the number variance for two different number of qubits (14 and 18), for the KIC. We find a very clear and notable difference: the data for the KIC tends to saturate at different, lower value of the unfolded spectral parameter $s_\infty \ll \mathcal{N}$, than COE, which typically saturate only at $s \sim \mathcal{N}/2$. Furthermore, the plateau is quite notorious. In the next plot (fig. 5) we have determined the saturation threshold s_∞ and the saturation value $\Sigma_\infty^2 = \Sigma^2(s_\infty)$ as a function of the number of qubits L .

Numerical results suggest that $s_\infty \approx 0.062\mathcal{N} \propto 2^L/L$, namely that s_∞ is proportional to \mathcal{N} though it is smaller by a large constant factor. The saturation value Σ_∞^2 thus increases logarithmically with \mathcal{N} , or linearly with L .

Perhaps a more clear picture is obtained after going into the time domain and inspecting the form factor K_2 for a few kicks, which correspond to large spectral ranges of Σ^2 . This regime is analogous to the non-universality regime corresponding to the shortest classical periodic orbit in quantum chaotic systems with well defined (semi)classical limit. However, we should not forget that our spin chain does not have any well defined classical limit or semi-classical regime. Still, it seems that $K_2(1/\tau_H)$, $K_2(2/\tau_H)$, etc., notably deviate from expectations of COE of the same dimensions as the KIC propagator. Indeed, in fig.6 we show $K_2(1/\tau_H)$ as a function of L , both for individual quasi-momentum k subspaces and the average over all relevant k , and find very clear and systematic deviation from COE expectation $K_{2,\text{COE}}(1/\tau_H) = 2/\mathcal{N}$. Furthermore, deviation of $K_2(1/\tau_H)$ is much bigger than expected COE fluctuation of $K_2(1/\tau_H)$ which can be computed as

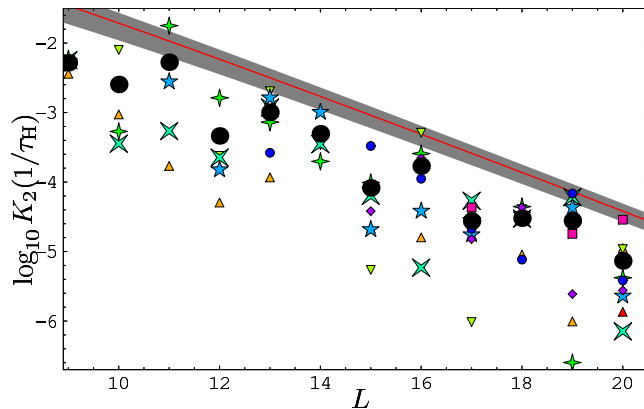


FIG. 6: We plot the value of K_2 evaluated at the first kick, for different quasi-momentum sectors (symbols according to fig. 3) and averaged over all quasi-momenta (filled circles). The red line indicates the theoretical COE value surrounded by one expected standard fluctuation (according to theoretical COE fluctuation) indicated by gray area. The average is systematically below the expected RMT value.

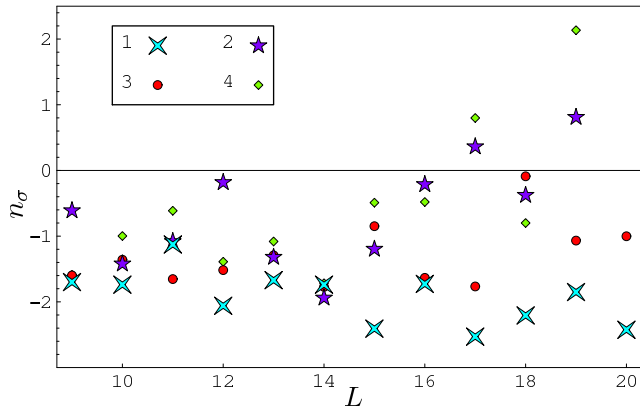


FIG. 7: We quantify here the number of standard deviations n_σ for which the value of the form factor of the KIC deviates from the RMT prediction. This calculations were performed for 1, 2, 3 and 4 kicks. The prominent feature is that for one kick we are always near 2 standard deviations away from the predicted result, systematically always undershooting the RMT result. For higher number of kicks the behavior is statistically as expected.

$$\sqrt{\langle K_2(1/\tau_H)^2 \rangle_{\text{COE}} - \langle K_2(1/\tau_H) \rangle_{\text{COE}}^2} = 2/\mathcal{N} + \mathcal{O}(\mathcal{N}^{-2}).$$
 Actually, in the limit $\mathcal{N} = \infty$, few higher moments can be computed as well and COE distribution of $K_2(1/\tau_H)$ is conjectured to be exponential. In fig. 7 we plot the relative deviation of $K_2(t/\tau_H)$, for $t = 1, 2, 3, 4$, from ex-

pected COE average in terms of the number of expected standard deviations. It is clear that, at least for one kick, the deviation is exceeding COE model significantly. Namely we find the deviation in the same direction for all different numbers of qubits L , and for almost all L it is exceeding two standard deviations. We also find statistically significant deviations from COE for other values of t , in particular for $t = 3$, while the deviations for even arguments $t = 2, 4$ are less clear and conclusive.

A specialized reader may inquire for a comparison with the DODO random matrix ensemble (which resembles semi-separable systems [10]). We note that the deviations from the COE observed in this article cannot be accounted by the semi-separable structure of the Floquet operator (3).

V. CONCLUSIONS

We have performed numerical calculations of large quasi-energy spectra of an interacting multi-qubit system, namely the kicked Ising chain. No analytical solution of the model is known, i.e. the model is believed to be non-integrable. Consistently with previous results in the literature [11], we find good agreement of short-range level statistics of the model with Dyson's ensemble of circular random matrices. However, when looking in detail at certain long-range spectral statistics, corresponding to short-times, we find notable and significant deviations from random matrix theory. This result reminds of non-universal regimes in semi-classical chaos widely studied in the 1990's. However, this behaviour cannot be attributed to periodic-orbits, since the system lacks any sensible definition of a classical limit.

We believe that the numerical results are intriguing and await for theoretical explanation, perhaps in the direction of suggesting a new, abstract semi-classical picture (perhaps along the lines of Ref.[12]).

Acknowledgments

We acknowledge discussion with T. H. Seligman and F. Leyvraz. We are grateful for many insights gained in discussions with C. Bunge and E. Brady. The work of C.P. was supported by Dirección General de Estudios de Posgrado (DGEP). T.P. acknowledges support from Slovenian Research Agency (program P1-0044 and Grant No. J1-7347). CP thanks the University of Ljubljana and its group for Nonlinear Dynamics and Quantum Chaos for hospitality.

[1] G. Casati, F. Valz-Gris and I. Guarneri, *Lett. Nuovo Cimento* **28**, 279 (1980); O. Bohigas, M.-J. Giannoni and

C. Schmit, *Phys. Rev. Lett.* **52**, 1 (1984).

- [2] M. L. Mehta, *Random Matrices* (Academic Press, San Diego, California, 1991), 2nd ed.
- [3] S. Müller, S. Heusler, P. Braun, F. Haake and A. Altland, Phys. Rev. Lett. **93**, 014103 (2004); Phys. Rev. E **72**, 046207 (2005).
- [4] M. V. Berry, Proc. R. Soc. London, Ser. A **400**, 229 (1985).
- [5] T. Prosen, Phys. Rev. E **60**, 3949 (1999).
- [6] T. Prosen, Phys. Rev. E **60**, 1658 (1999).
- [7] T. Prosen, Phys. Rev. E **65**(3), 036208 (2002).
- [8] B. Dietz and F. Haake, Z. Phys. B **80**, 153 (1990).
- [9] T. Prosen and M. Robnik, J. Phys. A **26**, 2371 (1993).
- [10] T. Prosen, T. H. Seligman, and H. A. Weidenmüller, Europhys. Lett. **55**(1), 12 (2001).
- [11] C. Pineda, R. Schafer, T. Prosen, and T. Seligman, Phys. Rev. E **73**(6), 066120 (2006).
- [12] K. S. Gibbons, M. J. Hoffman, and W. K. Wootters, Phys. Rev. A **70**, 062101 (2006).
- [13] F. Leyvraz, private communication, 2006.
- [14] R. Ketzmerick, K. Kruse, and T. Geisel, Physica D **131**, 247 (1999), cond-mat/9712209.
- [15] M. Berrondo, A. V. Bunge, and C. F. Bunge, Computers & Chemistry **10**, 269 (1986).

APPENDIX A: DIMENSIONS OF THE INVARIANT SUBSPACES

Consider the computational basis $S = \{|m_0 m_1 \dots m_{L-1}\rangle\}$, $m_j \in \{0, 1, \dots, d-1\}$ of the Hilbert space of L qudits $\mathcal{H} = \mathcal{H}_{\text{qudit}}^{\otimes L}$. Let us generalize the translation operator allowing the m_j 's to have integer values between 0 and $d-1$. The Hilbert space \mathcal{H} is foliated into L subspaces \mathcal{H}_k such that for any $|\psi\rangle \in \mathcal{H}_k$, $T|\psi\rangle = \exp(2\pi i k/L)|\psi\rangle$ and $\mathcal{H} = \bigoplus_{k=1}^L \mathcal{H}_k$. Let P_k be the orthogonal projection operator, such that $P_k|\psi\rangle \in \mathcal{H}_k$, for any $|\psi\rangle \in \mathcal{H}$. An elegant solution to the problem of calculating $\dim \mathcal{H}_k$ is presented here, following [13].

We first study the condition under which a state $|n\rangle \in S$ is projected to the null ket (zero vector). Let J be the smallest positive integer such that $T^J|n\rangle = |n\rangle$; we call J the primitive period of $|n\rangle$. The action of the projection operator P_k on $|n\rangle$ is

$$P_k|n\rangle = \left(\sum_{j=0}^{\frac{J}{L}-1} (\varphi_{J,k})^j \right) \left(\sum_{j=0}^{J-1} \varphi_{j,k} T^j \right) |n\rangle, \quad (\text{A1})$$

with $\varphi_{l,k} := e^{-2\pi i \frac{lk}{L}}$. Notice that $P_k|n\rangle = 0$ if and only if $\gamma = \sum_{j=0}^{\frac{J}{L}-1} (\varphi_{J,k})^j = 0$. Since γ is the sum of a geometric series, its calculation is straightforward: $\gamma = 0$ if and only if $\varphi_{J,k} \neq 1$. As a conclusion we obtain that $P_k|n\rangle \neq 0$ if and only if $\frac{kJ}{L} \in \mathbb{Z}$.

Define the equivalence relation \sim in S as: $|n\rangle \sim |m\rangle$ if there exists an integer j such that $|n\rangle = T^j|m\rangle$. Furthermore, if $|n\rangle \sim |m\rangle$, then $P_k|n\rangle \propto P_k|m\rangle$, but if $|n\rangle \not\sim |m\rangle$, then $\langle n|P_k^\dagger(P_k|m)\rangle = 0$. In other words, elements in different equivalence classes, are projected to orthogonal

states. Thus counting the equivalence classes which are not projected to 0 yields $\dim \mathcal{H}_k$.

Let $\tilde{N}(J)$ be the number of equivalence classes whose elements have given primitive period J . If we call $N(J)$ the number of elements in S that have primitive period J , then, $N(J) = J\tilde{N}(J)$. Notice that

$$\sum_{\{J|\frac{L}{J} \in \mathbb{N}\}} N(J) = \sum_{\{J|\frac{L}{J} \in \mathbb{N}\}} J\tilde{N}(J) = d^L \quad (\text{A2})$$

as the only allowed values for J are the divisors of L . Using Möbius inversion formula we obtain

$$\tilde{N}(J) = \frac{1}{J} \sum_{\{m|\frac{L}{m} \in \mathbb{N}\}} \mu\left(\frac{J}{m}\right) d^m. \quad (\text{A3})$$

Möbius function μ is defined over the positive integers as $\mu(1) = 1$, $\mu(n) = 0$ if n is divisible by the square of a prime, and in any other case, $\mu(n) = (-1)^p$ where p is the number of prime factors of n . Then, collecting our results,

$$\dim \mathcal{H}_k = \sum_{\{J|\frac{L}{J}, \frac{kJ}{L} \in \mathbb{N}\}} \tilde{N}(J) \quad (\text{A4})$$

since the only possible primitive periods J are the divisors of L . However the value of $\dim \mathcal{H}_k$ is well approximated by $2^L/L$ for large values of L .

APPENDIX B: THE OPTIMAL BASIS FOR DIAGONALIZATION OF KIC

To get the spectra used in this paper, it is crucial to develop an optimal diagonalization scheme. Though the techniques relying on Lanczos method [14] are fast they are not completely reliable. They loose precision as soon as some eigenvalues are close enough. In our experience the Lanczos method allows to obtain the full spectra for systems of up to 21 qubits, but the intrinsic numerical error becomes comparable to the mean level spacing. Even for 18 qubits, the biggest numerical error in one level is already bigger than the smallest inter-level spacing. As we are performing very precise tests we require that our levels are highly reliable, making Lanczos a prohibitively inexact method. We prefer using direct diagonalization with specialized routines [15].

Let $U_{s,\text{KI}} = U_{\text{kick}}(\vec{b}/2)U_{\text{Ising}}(J)U_{\text{kick}}(\vec{b}/2)$ be the symmetrized version of U_{KI} , which however has the same spectrum due to unitary equivalence. Using an appropriate basis is important both to take advantage of the natural block diagonal decomposition of $U_{s,\text{KI}}$ (due to symmetry P) and its symmetric character (due to symmetry \mathcal{K}). The basis is constructed as follows. Let $|n\rangle$ be a representative of a class defined by \sim (see App. A), and such that $P_k|n\rangle \neq 0$. If $\langle n|RP_k|n\rangle = 0$ then both $P_k|n\rangle \pm \mathcal{K}RP_k|n\rangle$ are used as members of the basis. If $\langle n|RP_k|n\rangle \neq 0$ at least one of $P_k|n\rangle \pm \mathcal{K}RP_k|n\rangle$ is not

the null ket, and can be incorporated into the base. By choosing $|n\rangle$ from all different classes we build a com-

plete basis in \mathcal{H}_k . Moreover, this basis is invariant under \mathcal{K} and is orthogonal.